

Numerical Simulation of Plasma Antenna with FDTD Method *

LIANG Chao(梁超)**, XU Yue-Min(徐跃民), WANG Zhi-Jiang(王之江)

Center for Space Science and Applied Research, Chinese Academy of Science, Beijing 100190

(Received 15 July 2008)

We adopt cylindrical-coordinate FDTD algorithm to simulate and analyse a 0.4-m-long column configuration plasma antenna. FDTD method is useful for solving electromagnetic problems, especially when wave characteristics and plasma properties are self-consistently related to each other. Focus on the frequency from 75 MHz to 400 MHz, the input impedance and radiation efficiency of plasma antennas are computed. Numerical results show that, different from copper antenna, the characteristics of plasma antenna vary simultaneously with plasma frequency and collision frequency. The property can be used to construct dynamically reconfigurable antenna. The investigation is meaningful and instructional for the optimization of plasma antenna design.

PACS: 52.25.Os, 52.40.Fd

Researchers have presented the proposal of using plasma as the conductor in an rf antenna and have paid attention to the concept of plasma antenna for years. In contrast to the conventional copper antenna, the plasma antenna has the advantages of switchable radar cross section, frequency and shape agility, dynamically reconfigurability characteristics.

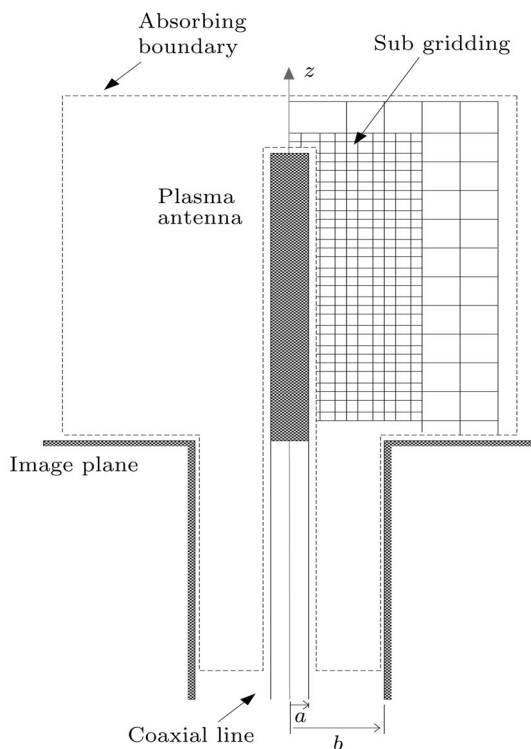


Fig. 1. FDTD geometry of plasma antenna fed through a coaxial transmission line.

Hettinger^[1] suggested that the ionized gas can be used to radiate and to receive wireless signals. In the 1960s, Askar'yan^[2] proved this prediction by experi-

ments. Kang *et al.*^[3] demonstrated a construction of an antenna with a glass tube filled with low-pressure gas. Measurements of efficiency and radiation patterns of plasma column antenna have been reported by Borg *et al.*^[4] Characteristics of the plasma antenna largely depend on the behaviour of an electromagnetic wave propagating in plasma. However, few analytical solutions of the plasma antenna have been carried out because the permittivity of plasma varies significantly with frequency. With rapid growth of computation speed, the finite-difference time-domain method offers an accurate way for simulating the interactions between plasma medium and radio wave, also predicting the characteristics of such antenna. With this method, Maloney *et al.*^[5] have already analysed radiation from simple copper antennas, and the computed results are in excellent agreement with accurate experimental measurements. Here, for the advantages of less amount of calculation and perfect mesh, we adopt cylindrical-coordinate JEC-FDTD algorithm to analyse a plasma antenna with column configuration.

Figure 1 shows the FDTD geometry of plasma antenna fed through an image plane from a coaxial transmission line, where the excitation voltage is introduced into. Since results over a wide bandwidth are desired, the antenna is excited with a transient pulse source voltage rather than the sinusoidal source. The incident wave used in the simulation is a Gaussian pulse whose frequency spectrum peaks at 24 GHz and is 10 dB down from the peak at 48 GHz. The geometric parameters that describe the monopole antenna are the length $L = 0.4\text{m}$ and the radius of the conductors of the coaxial line a and b . We set $b/a = 2.30$, which corresponds to a characteristic impedance of $50\ \Omega$ for the coaxial line. The FDTD problem space is 200×200 cells. The technique of sub-gridding algorithm is also introduced to accurately

*Supported by the National Natural Science Foundation of China for Distinguished Youth Scholar under Grant No 10705040.

**Email: leong.chao@gmail.com

render the small structure features of plasma. Two grid spacings are used: in the vicinity of the antenna: $\Delta r_1 = \Delta z_1 = 2.5$ mm, while in the distant region: $\Delta r_2 \approx 10\Delta r_1, \Delta z_2 \approx 10\Delta z_1$. The computation time interval is $\Delta t = \Delta z/(2c)$ to meet stable requirement. A five-layer perfectly matched layer (PML)^[6] boundary is set to simulate the infinite vacuum. As discussed in Refs. [7,8], the thin-wire model is adopted to treat the update equations related to the coaxial probe. The well-known plasma dispersion equation for unmagnetized plasma is

$$\varepsilon(\omega) = \varepsilon_0 \left(1 + \frac{\omega_p^2}{\omega(j\nu_e - \omega)} \right), \quad (1)$$

where the parameters $\omega_p = \sqrt{Ne^2/m\varepsilon_0} = 2\pi f_p$, ε_0 is the permittivity of free space, N is the plasma density, e is the electric charge, m is the mass of an electron, ν_e is the average collision frequency of electrons, and f_p is the inherent plasma frequency. Throughout the simulation, we use the plasma frequency f_p as a plasma parameter rather than the electron density N , since the former is preferably used in the FDTD formulation. Simulations are performed in several cases: the plasma frequency ($f_p = 3$ –10 GHz; the equivalent plasma density is $N = 1.1 \times 10^{11}$ – 1.2×10^{12} cm⁻³) and the collision frequency ($\nu_e = 0.1$ –1.5 GHz).

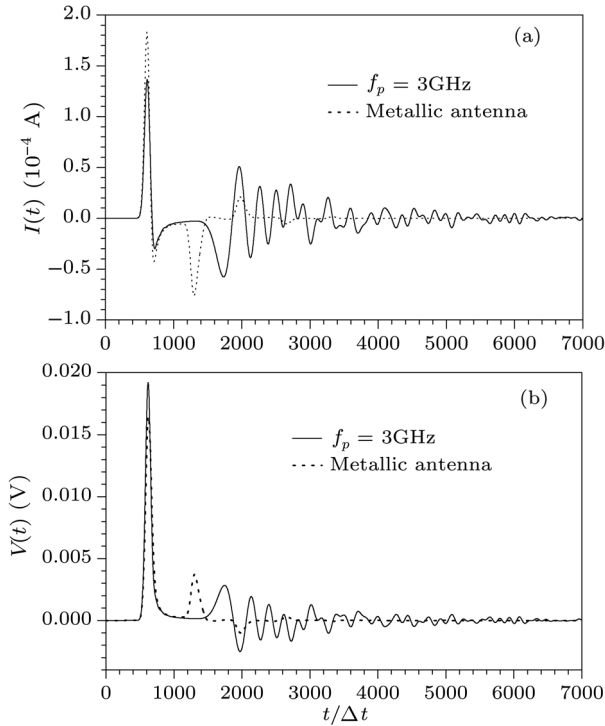


Fig. 2. $V(t)$ of metal antenna and plasma antenna with $f_p = 3$ GHz excited by a 1 V Gaussian pulse. (b) $I(t)$ of metal antenna and plasma antenna with $f_p = 3$ GHz excited by a 1 V Gaussian pulse.

According to the JEC-FDTD method,^[9] by per-

forming a backward-differencing approximation to Maxwell equations and plasma dispersion equation in cylindrical coordinates, a second-order approximation for numerical simulation can be derived for Yee's FDTD formulation as follows:

$$J_r|_{i,j-1/2}^{n+1/2} = e^{-\nu\Delta t} J_r|_{i,j-1/2}^{n-1/2} + \varepsilon_0 \omega_p^2 \Delta t e^{-\nu\Delta t/2} E_r|_{i,j-1/2}^n, \quad (2)$$

$$J_z|_{i+1/2,j}^{n+1/2} = e^{-\nu\Delta t} J_z|_{i+1/2,j}^{n-1/2} + \varepsilon_0 \omega_p^2 \Delta t e^{-\nu\Delta t/2} E_z|_{i+1/2,j}^n, \quad (3)$$

$$H_\phi|_{i,j}^{n+1/2} = H_\phi|_{i,j}^{n-1/2} + \frac{\Delta t}{\mu_0 \Delta r} [E_z|_{i+1/2,j}^n - E_z|_{i-1/2,j}^n] - \frac{\Delta t}{\mu_0 \Delta z} [E_r|_{i,j+1/2}^n - E_r|_{i,j-1/2}^n], \quad (4)$$

$$E_r|_{i,j-1/2}^{n+1} = E_r|_{i,j-1/2}^n - \frac{\Delta t}{\varepsilon_0 \Delta z} [H_\phi|_{i,j}^{n+1/2} - H_\phi|_{i,j-1}^{n+1/2}] - \frac{\Delta t}{\varepsilon_0} J_r|_{i,j-1/2}^n, \quad (5)$$

$$E_z|_{i+1/2,j}^{n+1} = E_z|_{i+1/2,j}^n + \frac{\Delta t}{\varepsilon_0 \Delta r} \frac{1}{\Delta r_{i+1/2}} [\Delta r_{i+1} H_\phi|_{i+1,j}^{n+1/2} - \Delta r_i H_\phi|_{i,j}^{n+1/2}] - \frac{\Delta t}{\varepsilon_0} J_z|_{i+1/2,j}^n. \quad (6)$$

In order to calculate the input impedance of plasma antenna, we record time-domain output of voltage $V(t)$ and current $I(t)$ at the antenna input port during the simulation. Figure 2 shows $V(t)$ and $I(t)$ of metal antenna and plasma antenna with $f_p = 3$ GHz excited by a 1 V Gaussian pulse. For copper antenna, we note that the peaks in the output data are spaced by about the round-trip transit time for the pulse on the antenna. However, because of particular dispersion pattern of plasma media, the output data for plasma antenna is not to be regular. These time-domain results are subsequently converted to the frequency-domain $V_A(\omega)$ and $I_A(\omega)$ using the FFT. The complex transforms are divided at each frequency to obtain the input impedance of the antenna,^[10]

$$Z_A(\omega) = V_A(\omega)/I_A(\omega). \quad (7)$$

Figure 3 shows the simulated antenna impedances for copper antenna and plasma antenna with different f_p (3, 4, 5, 10 GHz) while $\nu_e = 150$ MHz. We note that as the plasma frequency increases, the resonance characteristics of input impedance gradually approach to the situation of copper antenna. The resonant frequencies of plasma antenna are 129, 147, 158, 180 MHz respectively, and 193 MHz for copper antenna. Most importantly, the lower quantity of f_p , the higher quantity of antenna's Q-factor, which means that the input impedance is more sensitive to the radio wave frequency. Figure 4 shows the collision frequency's impact on input impedance. Different ν_e are considered,

which are 0.1, 0.5, 1, 1.5 GHz while $f_p = 5$ GHz. The lower quantity of ν_e , the higher antenna's Q-factor. However, ν_e does not influence the period of resonant behaviour. These properties can be used to construct dynamically reconfigurable antenna, in which the operating frequency can be varied by varying the plasma frequency and collision frequency. In the experimental situation, these are the gas pressure and the rf power applied to create plasma.

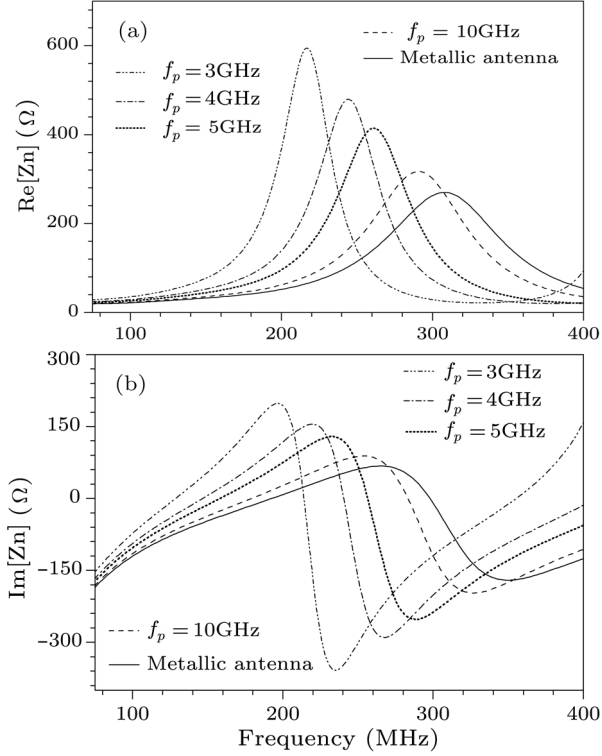


Fig. 3. (a) Real part of input impedances of metallic antenna and plasma antenna with $f_p = 3, 4, 5, 10$ GHz. (b) Imaginary part of input impedances of copper antenna and plasma antenna with $f_p = 3, 4, 5, 10$ GHz. The collision frequency is 150 MHz, the copper antenna and plasma antenna are with the same size.

In order to obtain the radiation efficiency of plasma antenna, three steps should be applied. Firstly, the input power is calculated in the usual way,

$$P_{in}(\omega) = \text{Re}[V_A(\omega)I_A^*(\omega)]. \quad (8)$$

Secondly, the radiated power is calculated through the integration of the far-field electric, which is derived with the method of far-zone transformation^[7],

$$P_{rad}(\omega) = \iint \frac{|E_F(\omega, \theta, \phi)|^2}{2\eta_0} \sin(\theta) d\theta d\phi, \quad (9)$$

where $E_F(\omega, \theta, \phi)$ is the Fourier transform of far-field electric with θ and Φ angles, η_0 is the characteristic impedance of vacuum. Finally, the efficiency $E_{\text{efficiency}}$ is obtained by the deduction of radiated power and in-

put power,

$$E_{\text{efficiency}}(\omega) = \frac{P_{rad}(\omega)}{P_{in}(\omega)}. \quad (10)$$

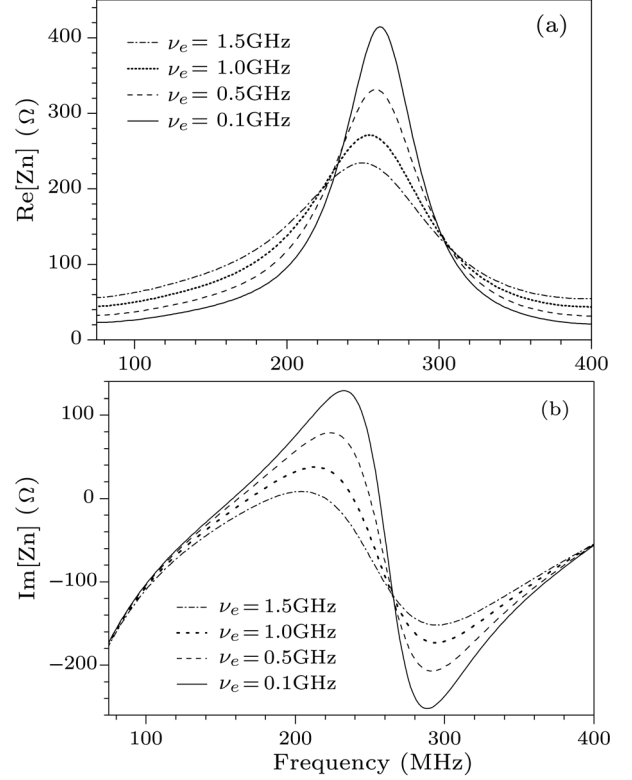


Fig. 4. (a) Real part of input impedances of plasma antenna with $\nu_e = 0.1, 0.5, 1.0, 1.5$ GHz. (b) Imaginary part of input impedances of plasma antenna with $\nu_e = 0.1, 0.5, 1.0, 1.5$ GHz. The plasma frequency is 5 GHz, the copper antenna and plasma antenna are with the same size.

Figure 5 (a) shows the radiation efficiency of plasma antenna compared with copper antenna. We set $f_p = 3, 5, 10$ GHz while $\nu_e = 150$ MHz and frequencies between 75 MHz to 1 GHz are investigated. We notice that as the plasma frequency increases, the efficiency approaches the situation of copper antenna. The efficiencies of the plasma antenna at lower frequencies (f/f_p) resemble those of a copper antenna, which also demonstrates the phenomenon that if $f \ll f_p$, plasma antenna can be treated as a copper antenna of the same configuration. Figure 5(b) shows the collision frequency's impact on radiation efficiency. Different ν_e are considered, which are 0.1, 0.5, 1, 1.5 GHz while $f_p = 5$ GHz. The result shows the higher the quantity of ν_e , the lower the efficiency at the same wave frequency. This is because the main interaction between plasma and radio wave is collisional absorption. The absorption of plasma to microwave is increased with the enhancement of the plasma collision frequency.^[11] The radiation efficiency varies with the parameters of f_p and ν_e , which offers

us the capability of efficiency management.

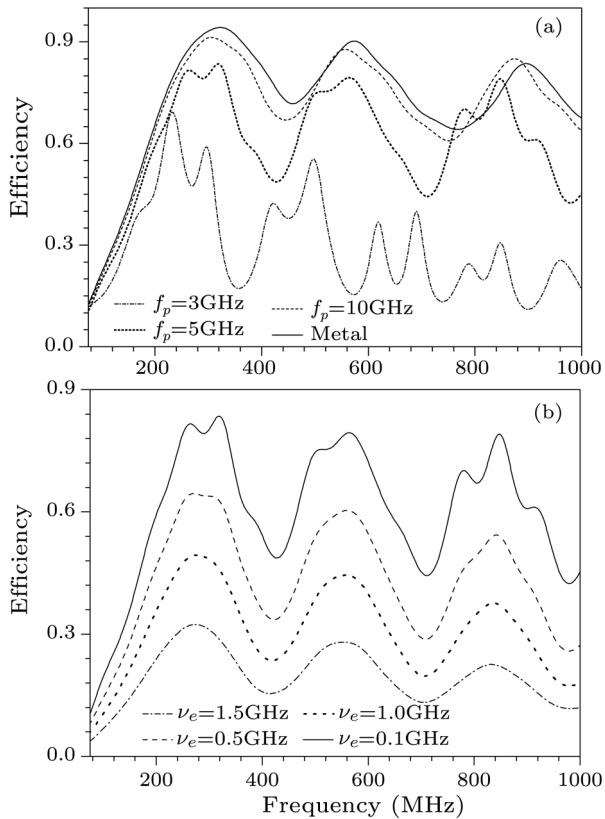


Fig. 5. (a) Radiation efficiency of copper antenna and plasma antenna with $f_p = 3, 5, 10$ GHz and $\nu_e = 150$ MHz. (b) Radiation efficiency of plasma antenna with $\nu_e = 0.1, 0.5, 1.0, 1.5$ GHz and $f_p = 5$ GHz.

In conclusion, we have studied the input impedance and radiation efficiency of a 0.4-n-long

column configuration plasma antenna based on the FDTD method, and the particular characteristics of these parameters are analysed. In our simulation, as f_p increases, the characteristics of the plasma antenna approach these of a copper antenna. The antenna impedance of plasma antenna shows clear resonant behaviour when f/f_p is low. Both f_p and ν_e can be altered to construct dynamically reconfigurable antenna. In addition, the collision frequency and the density of electrons in plasma significantly influence the radiation efficiency. As a result, to be a practical antenna, on the premise of the higher radiation efficiency, we could choose certain parameters of plasma to determine the operation frequency.

References

- [1] Hettlinger J 1919 *U.S. Patent No. 1309031*
- [2] Askar'yan G A 1965 *Sov. Phys. Tech. Phys.* **35** 1275
- [3] Kang W L, Rader M, and Alexeff I 1996 *Proceedings of the 1996 IEEE International Conference on Plasma Science* (Boston, 3–5 June 1996) p 261
- [4] Borg G G et al 2000 *Phys. Plasmas* **7** 2198
- [5] Maloney J G, Smith G S, and Scott Jr W R 1990 *IEEE Trans. Antennas Propagat.* **38** 1059
- [6] Guo X F, Qing H L 2000 *IEEE Trans. Antennas Propagat.* **48** 5
- [7] Kunz K and Luebbers R J *The Finite Difference Time Domain Method for Electromagnetics* (Boston: Artech House)
- [8] Taflov A and Hagness S C *Computational Electrodynamics: The Finite-Difference Time-Domain Method* (New York: CRC Press)
- [9] Qing C, Katsurai M and Aoyagi P H 1998 *IEEE Trans. Antennas Propagat.* **46** 1739
- [10] Stutzman W L, Thiele G A *Antenna Theory and Design* (New York: Wiley)
- [11] Stix T H *Waves in Plasmas* (New York: AIP)